Excited-state charge transfer dynamics in systems of aromatic adsorbates on TiO_2 studied with resonant core techniques

J. Schnadt[a] and J. N. O'Shea[b]
Department of Physics, Uppsala University, Box 530, 751 21 Uppsala, Sweden

L. Patthey
SLS, Paul Scherrer Institut, 5232 Villigen-PSI, Switzerland

L. Kjeldgaard, J. Åhlund, K. Nilson, and J. Schiessling
Department of Physics, Uppsala University, Box 530, 751 21 Uppsala, Sweden

J. Krempaský and M. Shi
SLS, Paul Scherrer Institut, 5232 Villigen-PSI, Switzerland

O. Karis
Department of Physics, Uppsala University, Box 530, 751 21 Uppsala, Sweden

C. Glover
MAX-Lab, University of Lund, Box 118, 221 00 Lund, Sweden
and Department of Physics, Uppsala University, Box 530, 751 21 Uppsala, Sweden

H. Siegbahn
Department of Physics, Uppsala University, Box 530, 751 21 Uppsala, Sweden

N. Mårtensson
MAX-Lab, University of Lund, Box 118, 221 00 Lund, Sweden
and Department of Physics, Uppsala University, Box 530, 751 21 Uppsala, Sweden

P. A. Brühwiler[c]
Department of Physics, Uppsala University, Box 530, 751 21 Uppsala, Sweden
and EMPA, Lerchenfeldstrasse 5, 9014 St. Gallen, Switzerland

(Received 26 February 2003; accepted 19 September 2003)

Resonant core spectroscopies are applied to a study of the excited electron transfer dynamics on a low-femtosecond time scale in systems of aromatic molecules (isonicotinic acid and bi-isonicotinic acid) adsorbed on a rutile $TiO_2(110)$ semiconductor surface. Depending on which adsorbate state is excited, the electron is either localized on the adsorbate in an excitonic effect, or delocalizes rapidly into the substrate in less than 5 fs (3 fs) for isonicotinic acid (bi-isonicotinic acid). The results are obtained by the application of a variant of resonant photoemission spectroscopy. © *2003 American Institute of Physics.* [DOI: 10.1063/1.1586692]

I. INTRODUCTION

Electron transfer plays a fundamental role in a wide field of chemical as well as biological systems. For instance, such transfer reactions are responsible for the functioning of photographical and lithographical techniques, for the generation of electrical power with solar cells, and for many enzyme-catalyzed reactions in biological systems. Traditionally, measurements of the electron transfer have been limited to static methods, i.e., methods that describe the outcome of, rather than the dynamical process itself. Time-resolved femtosecond (fs) techniques have in recent years enabled investigations on the true time scale of these processes, at least down to approximately 20 fs. However, in strongly bonded systems the transfer might occur at even shorter times, and some systems of this type show promise of being important from a technological point of view.

A class of systems that has been studied extensively is that of various chromophores attached to a nanostructured titanium dioxide substrate, forming the core of the potentially very interesting so-called ''dye-sensitized solar cell.''[1] These cells offer a unique combination of low fabrication costs, long lifetime, and high light-harvesting efficiency. Crucial for the high efficiency is (among other factors) a very rapid excited electron transfer from the chromophore to the substrate. The dye that has been found to yield the highest transfer rates to-date is[2] ''N3'' or $(dcb)_2Ru(NCS)_2$ (dcb=4,4′-dicarboxy-2,2′-bipyridine, which is also termed bi-isonicotinic acid, cf. Fig. 1), which binds to the nanostructured electrode via one or two dcb ligands. Upper limits in the range of 25–100 fs for the transfer times have been measured with the help of femtosecond laser techniques.[3–8] For the model system of dcb on rutile $TiO_2(110)$ characterized in Ref. 9, we reported recently[10] that the strength of the ligand-

[a]Author to whom all correspondence should be addressed; electronic mail: achim@phys.au.dk. Present address: Department of Physics and Astronomy, University of Aarhus, Ny Munkegade, 8000 Aarhus C, Denmark.
[b]Present address: School of Physics and Astronomy, University of Nottingham, Nottingham NG7 2RD, United Kingdom.
[c]Electronic mail: paul.bruehwiler@empa.ch

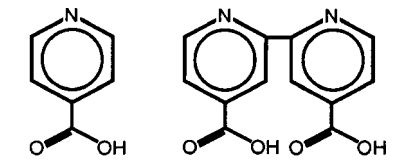

FIG. 1. The chemical structures of isonicotinic acid and bi-isonicotinic acid.

substrate bond allows for charge transfer times of less than 3 fs. This was achieved by employing resonant photoemission spectroscopy (RPES),[11] and it was the first study to show that such rapid charge transfer occurs for a relatively complex molecule adsorbed on a semiconductor, with a time approaching that of CO adsorbed on metal surfaces.[12,13]

In the present article we provide further details of the previous work[10] as well as new results for a related system [isonicotinic acid on rutile $TiO_2(110)$]. A primary development which is detailed in this paper is the application of a new variant of resonant photoemission to fs charge transfer.[10] As detailed in Ref. 13, the preferred approach in using resonant core spectroscopies to study dynamic charge transfer is to determine the ratio between the resonant and nonresonant portions of the decay spectra upon core level excitation of the species being probed, with several excellent recent examples.[12,14,15] This is, however, a challenge when there are other strong contributions to the spectrum from a substrate, e.g., especially when either of the two portions of interest are weak.[12,13,16] Another issue is the variable cross section of such background contributions as a function of photon energy, which can make their subtraction from the spectrum difficult to achieve without introducing large errors. An alternative approach is to focus on the resonant photoemission channels, which often minimizes the problems with strong interfering backgrounds.[13,16,17] Here, following Ref. 10, we adopt this approach, using finely spaced, moderate to high resolution excitation to be able to disregard the effects of the slowly varying direct photoemission background, and to be able to detect any effects of interference between the core-excited and directly-excited channels via a Fano-type profile.[13,15] We then apply the method to a new system, isonicotinic acid on $TiO_2(110)$ (cf. Fig. 1), which has recently been characterized structurally, and is found to exhibit noncovalent interaction between neighboring adsorbates, thus providing an interesting comparison to the case of the covalent dimer.[18,19]

As a supplement to the RPES method, an application of resonant Auger electron spectroscopy (RAES)[11] to the bi-isonicotinic acid system is discussed. The RAES approach is similar to that of, e.g., Refs. 20 and 21. In principle, RPES and RAES are able to give the same information on the charge transfer dynamics, and their distinction is less experimental than interpretational, since both methods rely on very similar data sets. We find that the RPES data are easier to interpret for relatively complex systems such as the present ones. Finally, a thorough discussion is included of how these results bear on the solar cell systems.

II. EXPERIMENT

The x-ray absorption spectroscopy (XAS) and RPES/RAES experiments were carried out at beamlines I511[22] and D1011[23] at the Swedish synchrotron radiation facility MAX-Lab in Lund. The samples were held in a Ta sample holder designed to maintain good thermal and electrical contact without stressing the sample. They were prepared *in situ* under ultra high vacuum conditions with a base pressure in the low 10^{-10} Torr range in the preparation chambers and in the low 10^{-11} Torr range in the analysis chambers. The rutile $TiO_2(110)$ crystals, purchased from Djévahirdjian, Industrie de Pierre Scientifique in Monthey, Switzerland, and from MaTecK, Jülich, Germany, were annealed in 1×10^{-6} Torr O_2 at high temperatures (700 °C) in order to make them conducting by the introduction of bulk defects. The surface was then cleaned by cycles of repeated Ar sputtering and annealing in a 1×10^{-6} Torr oxygen (99.999%) atmosphere at temperatures between 570 and 700 °C.

Isonicotinic acid was obtained from Sigma-Aldrich and bi-isonicotinic acid from Solaronix, Switzerland. They were outgassed thoroughly in a thermal sublimation stage, which was connected to the preparation chamber via a manual valve and equipped with a separate turbomolecular pump and pressure and temperature monitors. For sublimation the stage could be brought close to the TiO_2 crystal. The powder temperature during deposition was approximately 90 °C for isonicotinic and 230 °C for bi-isonicotinic acid. The substrate was kept at 200 °C for monolayer preparations and at room temperature (bi-isonicotinic acid) and around −100 °C (isonicotinic acid), respectively, for multilayers. For the monolayer preparations the coverage could be deduced from the intensities of the molecular and substrate O 1*s* peaks in the photoemission spectra. The observed intensity ratio corresponded approximately to a saturated monolayer.

The x-ray absorption spectra were recorded either in the partial-yield mode with a retardation voltage of −320 V on the detector (bi-isonicotinic acid) or they were obtained by integrating the valence spectra over the complete recorded range in the RPES/RAES measurements (isonicotinic acid), which corresponds to a measurement of the XAS in the Auger-yield mode. The photon energies of the x-ray absorption spectra and the resonant photoemission spectra were calibrated by measuring the kinetic energy difference of a core level photoemission line in first and second order. For the purpose of imaging the core-excited density of states they were further put onto the same scale as the photoemission spectra as outlined in Refs. 13 and 24. The kinetic energy scale of the normal Auger spectrum was calibrated by referencing it to the calibrated kinetic energy of a characterized core level.

The photon energy resolution was 90 meV in the RPES experiments on isonicotinic acid and the bi-isonicotinic acid multilayer and 60 meV in the bi-isonicotinic acid monolayer RPES experiment. The photon energy step was 0.1 eV (0.15 eV) in the bi-isonicotinic acid (isonicotinic acid) monolayer RPES and 0.2 eV in the multilayer RPES measurements. For the RAES experiment the resolution was set to 0.3 eV; the photon energy resolutions employed in the measurements of the x-ray absorption spectra are given in the figure captions.

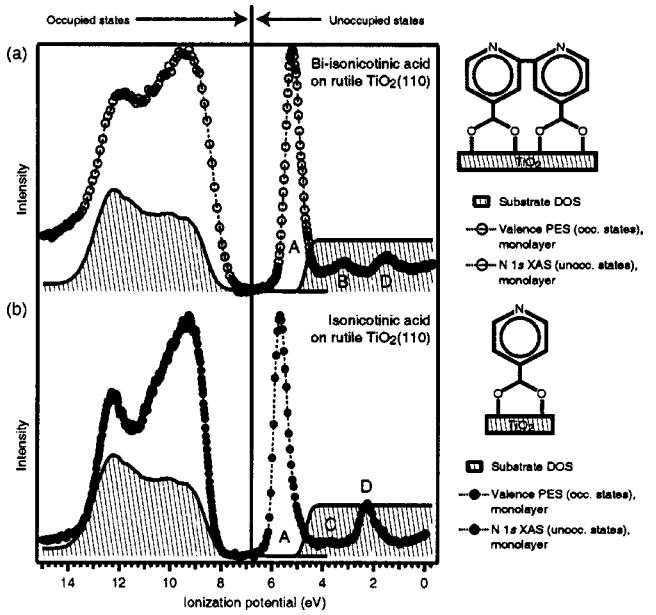

FIG. 2. Density of states, as probed by photoemission sepctroscopy and x-ray absorption spectroscopy, relevant to an excited electron transfer in monolayers of (a) bi-isonicotinic acid and (b) isonicotinic acid on $TiO_2(110)$. The photon resolution employed during the XAS measurements was 120 meV.

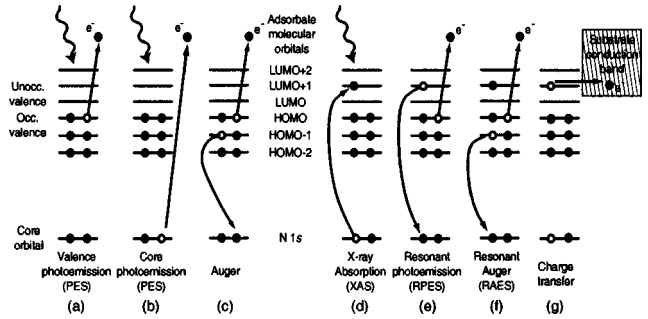

FIG. 3. Experimental methods. The diagrams depict schematically the electronic states of an isolated molecular system. The states are labeled HOMO (highest occupied molecular orbital), HOMO−1, etc., and LUMO (lowest unoccupied molecular orbital), LUMO+1, etc. Since the XAS and RPES/RAES measurements were performed using the N 1*s* core level, this is the only core level indicated here. In panel (g) this isolated system is coupled to a substrate, which allows for an electron transfer if the electronic matching condition is fulfilled.

III. DENSITY OF STATES

The key to an understanding of the charge transfer dynamics in a heterogeneous semiconductor system is the electronic structure. A necessary condition for a charge transfer on the low-fs time scale is that the donor state is energetically matched by an acceptor state. For low-femtosecond charge transfer events upon core-excitation as examined here, the donor state is not relaxed and it is the core-excited electronic state as measured in the x-ray absorption that is relevant for the donor state of the charge transfer process. On the opposite side it is the transport density of states (DOS) of the substrate that plays the role of the acceptor. Experimentally, this transport DOS can be assessed by inverse photoemission spectroscopy. Reliable data from this method are, however, often not readily available. An alternative route is to use calculations of the ground state density of states instead, since they often are closely related to the transport DOS.[25] A simpler approach is chosen here, which estimates the onset of the substrate unoccupied states from the size of the optical band gap (see the following).

An electronic state distribution that combines the molecular core-excited DOS as measured in the XAS with the substrate DOS is presented in Fig. 2 for isonicotinic acid and bi-isonicotinic acid. The procedures and concepts underlying such an arrangement are described in Refs. 10, 13, and 24. The occupied DOS was probed by valence photoemission for both the clean and monolayer-covered $TiO_2(110)$ surfaces. The valence band edge of the clean surface spectrum allows one to estimate the onset of unoccupied substrate states by taking the optical gap into account (3.1 eV for rutile TiO_2, Ref. 26).

Considering Fig. 2 with this in mind, it is seen that the lowest unoccupied state probed in XAS (resonance A) lies within the substrate bandgap, while the two following higher resonances (C and D for isonicotinic acid, and B and D for bi-isonicotinic acid) overlap the substrate DOS. Hence, an electron transfer event is electronically forbidden for excitation to the LUMO (lowest unoccupied molecular orbital, which is resonance A), while it is allowed for the higher resonances. This assessment does not give any information about whether charge transfer actually will occur from the higher resonances (since other properties of the core-excited system such as spatial overlap and conservation of angular momentum play in), but it indicates that such an event is energetically allowed,[10,13] a topic which is further examined in Sec. IV.

Principally important for this arrangement is the question of whether the unoccupied DOS of the substrate contains another gap (or depletion of the DOS) approximately 2–3 eV above the conduction band edge. Such a gap has been predicted by calculations,[10,27–29] but experimentally the situation is less clear-cut, with only a moderate decrease in the density of states as assessed using XAS[30,31] and inverse photoemission.[32] Judging from the data presented in the following such a gap is at least not evident at the positions of the higher resonances of the adsorbates.

IV. RESONANT PHOTOEMISSION AND RESONANT AUGER

The basic spectroscopic processes considered here are sketched in Fig. 3. Panels (a) and (b) show ordinary valence and core electron photoemission and panel (c) depicts the Auger decay that occurs upon core ionization. In panel (d) the process of core excitation is sketched, which is the process underlying x-ray absorption spectroscopy. Panels (e) and (f) contain the (resonant) decay channels upon core excitation, while panel (g) shows an adsorbate-to-substrate charge transfer of the excited electron. Thus the process of panel (d) is the step preceding the processes of panels (e), (f), and (g). In this picture we have to chosen to apply a two-step description, in which the excitation is separated from the deexcitation. Strictly, such a description is correct only if these two processes are decoherent (see, e.g., Ref. 33), which

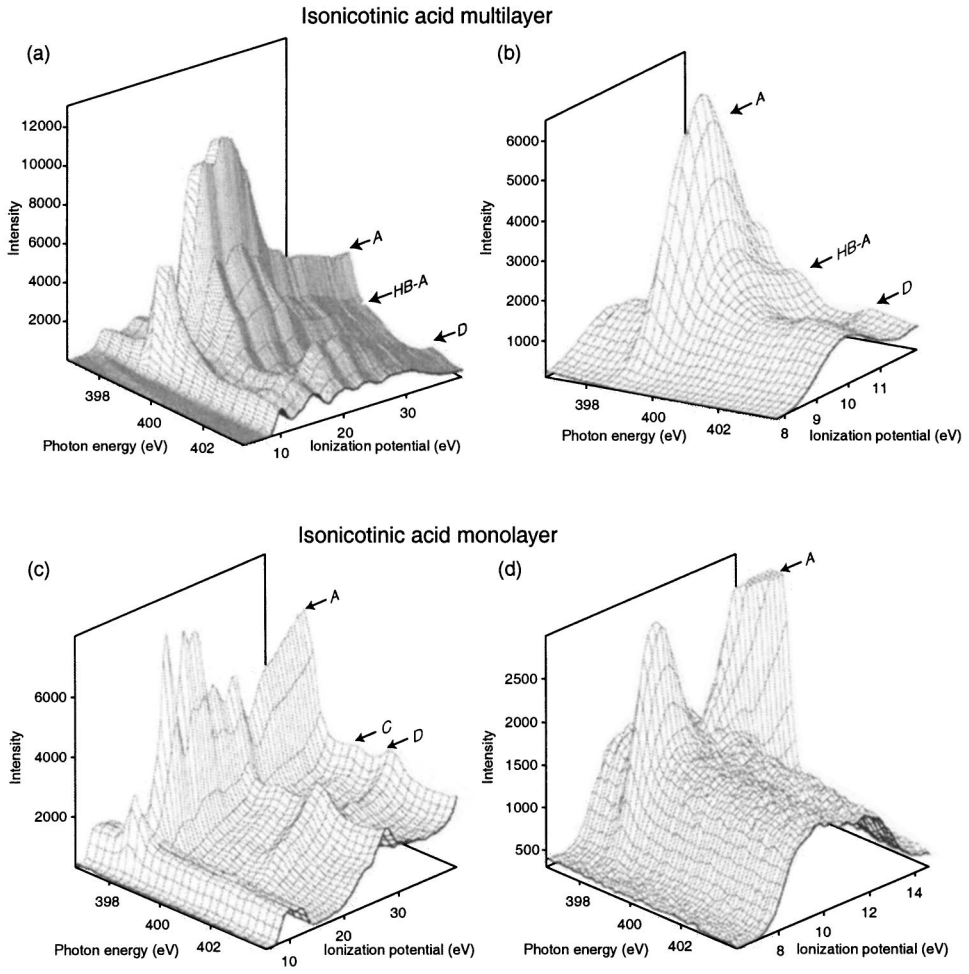

FIG. 4. RPES/RAES spectra for an isonicotinic acid multilayer [(a) and (b)] and a monolayer of isonicotinic acid on rutile $TiO_2(110)$ [(c) and (d)]. (b) and (d) A closer view of the low binding-energy data in (a) and (c), respectively. The labels A, C, D, and HB-A refer to the unoccupied states observed in the x-ray absorption spectra (cf. Figs. 2, 5, and 6).

is generally true for broad-band excitation with photon bandwidths larger than the lifetime broadening of the excited state or, as further outlined in the following, if the coherence is destroyed by, e.g., an excited-electron transfer from the adsorbate into the substrate. The argumentation in the following is therefore valid independent of whether a two-step or a one-step description is chosen.

From Figs. 3(a) and 3(e) it is noted that the final state of direct valence photoemission and resonant photoemission is the same, while the resonant Auger state corresponds to a shake-up state (the resonant Auger decay is often termed spectator decay due to the fact that the excited electron does not take part in the decay process).[11] Hence, the resonant photoemission signal has a constant binding energy independent of the photon energy as does that of the valence photoemission, and both occur at the same binding energy. In contrast, the resonant Auger signal stays at constant kinetic energy as does the normal Auger signal. An exception from this behavior occurs when employing the so-called Auger resonant Raman condition,[34] for which the photon bandwidth is chosen to be much smaller than the lifetime broadening of the excited state. Then the resonant Auger signal also disperses linearly with the photon energy (on a kinetic energy scale), i.e., it stays at constant binding energy.[12–14] This is valid as long as the excitation energy is varied within a single excitation resonance only. Over the entire regime of interest, which in the present case comprises three resonances, the overall change in kinetic energy is practically negligible for the resonant Auger signal (see the discussion in Sec. IV C). Hence, the different (overall) dispersion behavior allows one to distinguish between the two resonant decay channels.

The resonant signal (plus the nonresonant Auger signal) is recorded by measuring the valence photoemission spectrum at the resonant photon energies relevant for the x-ray absorption. This is illustrated in Fig. 4, which in panels (a) and (b) contains the resonant photoemission/resonant Auger data for a multilayer of isonicotinic acid and in panels (c) and (d) for a monolayer of isonicotinic acid on $TiO_2(110)$ [(b) and (d) merely give an expanded view of the highest occupied states]. In these images, structures are observed parallel to the photon energy axis that are (almost) constant in intensity. These stem from direct valence photoemission, and the resonant signal is superposed onto them. In principle, both channels could interfere leading to a Fano profile behavior along the photon energy axis;[13,15] this is, however, not observed here.

Qualitatively, when scanning the photon energy, the resonant intensity follows that of the x-ray absorption spectra (cf. Figs. 5 and 6). An important exception to this behavior is the low-binding energy region of Fig. 4(c) or, equivalently, the data set of panel (d). There, a resonant intensity is only detected for excitation to resonance A, but not to resonances C and D. The overall analogy of XAS and RPES/RAES,

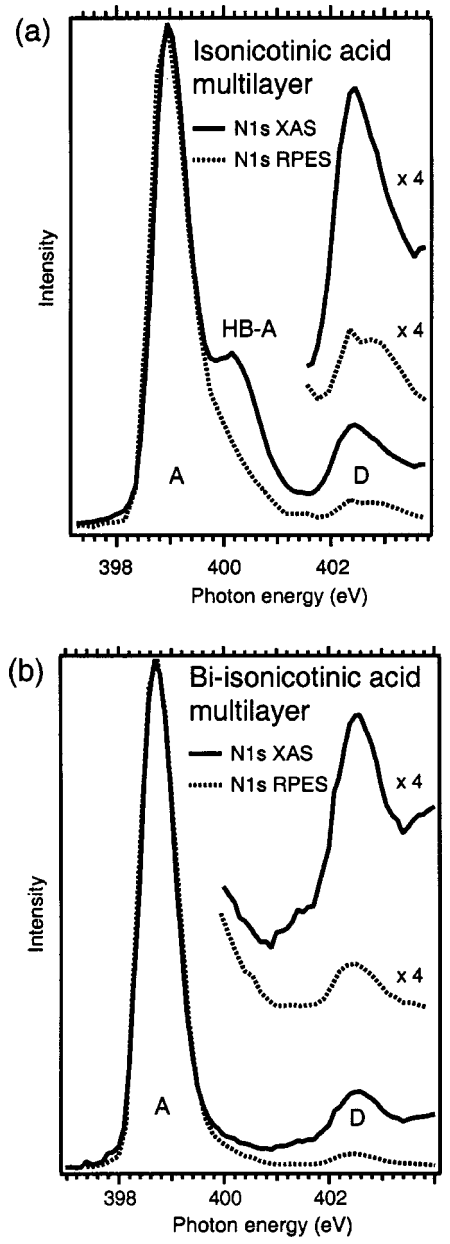

FIG. 5. Multilayer resonant photoemission spectra in comparison to the XAS for (a) isonicotinic acid and (b) bi-isonicotinic acid. The original data as presented in Fig. 4(b) were integrated for each photon energy resulting in the present curve in panel (a). An equivalent procedure was applied to the original bi-isonicotinic acid data not shown here. The photon energy resolution of the XAS measurements was 90 meV.

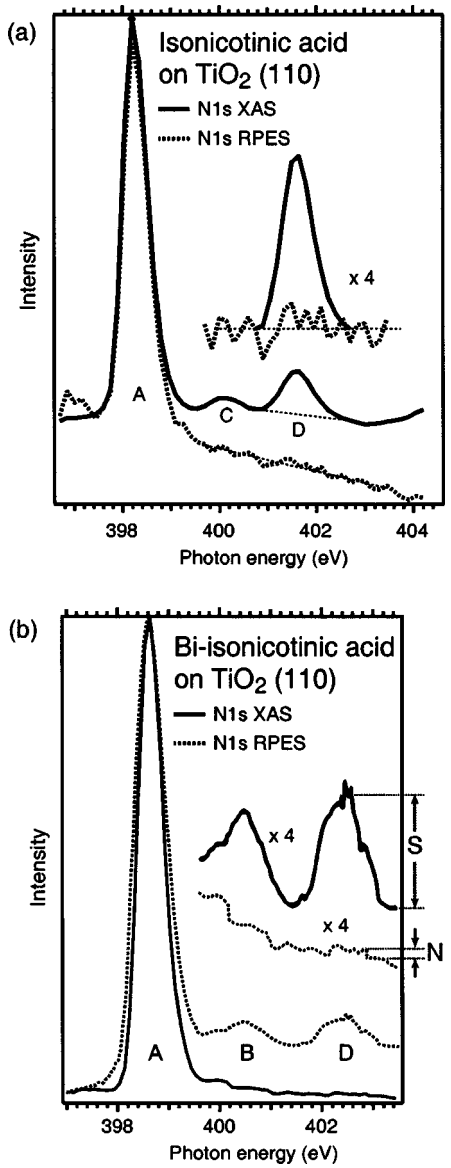

FIG. 6. Monolayer resonant photoemission curves in comparison to the XAS for (a) isonicotinic acid and (b) bi-isonicotinic acid on TiO_2(110). As in Fig. 5 the RPES curves are here given in their integrated form. The photon resolution of the x-ray absorption spectra was set to (a) 90 meV and (b) 150 meV.

which is expected since the number of electronic decays (normal Auger+resonant Auger+resonant photoemission) is proportional to the absorption cross section, has been indicated in the figure by labeling the unoccupied states accordingly.

If the core-excited molecule is coupled to a substrate, an excited electron charge transfer channel might compete with the resonant decay channels and alter the spectral appearance. The transfer process has been schematically indicated in Fig. 3(g). The resulting core-excited state is the same as the one produced in a core photoemission event [panel (b) of Fig. 3] and decays in an Auger decay depicted in panel (c). If the charge transfer time scale is much shorter than that of the decay, the resonant decay channels (e) and (f) are completely quenched. In the more general case, the resonant signal is reduced in intensity (while still observable), and the normal Auger peak gains in intensity, as the transfer time is shortened.[13] The resonant Auger decay of Fig. 3(f) can then be distinguished from that of the normal Auger channel by its so-called spectator shift to higher kinetic energy and/or by the linear Auger Resonant Raman shift.[12–14] The spectator shift is caused by the additional screening provided by the core-excited electron in comparison with the normal Auger.

The absence of any resonant photoemission signal for the higher resonances (C and D) of the isonicotinic acid monolayer in panel (d) of Fig. 4 is explained by a total quenching of the resonant photoemission as described for cases (e) and (f) above. Thus, the excited electron is rapidly delocalized into the substrate. The most reliable way of

quantifying the extent of delocalization or localization of the excited electron on the time scale of the core-hole lifetime would be to identify the branching ratios of the resonant and nonresonant channels in the spectra[12,13,21,35] (for each unoccupied state separately), corresponding to a localization and a delocalization, respectively. In Sec. IV C it will be shown that such a differentiation is very difficult for the present systems with a complex valence electronic structure and large substrate signal. Alternatively, an isolated system with no charge transfer can be used to normalize the intensities of the corresponding coupled system.[10,13,16,17] Then it is sufficient to take into account only the easily resolved resonant photoemission features that occur at the low-binding energy end of the spectrum. Since we are dealing with gap systems, it is ensured that these peaks contain no other signal with the exception of the direct valence photoemission, which constitutes a slowly varying background (as a function of photon energy). A quantification is then achieved by integrating the spectral intensity of the resonant peaks for each photon energy. This approach will be discussed in the following two sections.

A. Multilayer resonant photoemission

In Fig. 5(a) the resonant photoemission data from Fig. 4(b) are replotted in integral form. For each photon energy the spectral intensity was integrated between 9.15 and 10.65 eV binding energy[36] which resulted in the N $1s$ RPES curve in Fig. 5. There the latter is compared to the N $1s$ x-ray absorption spectrum. Panel (b) contains the corresponding data for a multilayer of bi-isonicotinic acid. The XAS of isonicotinic acid contains three resonances, the LUMO (peak A), the LUMO of the hydrogen-bonded species[37,38] in the bulk of the film (peak HB-A) and the LUMO+1 (peak D). Due to the particular choice of preparation conditions, hydrogen bonding does not occur to a significant extent in the bi-isonicotinic acid multilayer, and thus only two peaks A and D are found.

Both the x-ray absorption and the resonant photoemission spectra were normalized to the height of peak A. This procedure corresponds to an intensity calibration of the RPES signal to that of the x-ray absorption spectrum. For the higher resonances HB-A and D the intensity follows that of the XAS, but is clearly reduced by approximately a factor of 3. While this could indicate delocalization of the excited electrons in these resonances, we judge that such a process is rather unlikely due to the van der Waals nature of the films. In addition, the electronic matching condition of Sec. III is not easily fulfilled in a molecular crystal with discrete states, since the local perturbation by a core-hole leads to a change in electronic structure similar to the above-reported excitonic effect. Thus the lowest resonance A lies certainly within the molecular gap of the surrounding medium,[13] and, similarly, this is also likely for the higher resonances due to the discrete nature of the molecular states. For these reasons, the decrease in RPES cross section compared to that of the lowest resonance is rather attributed to a reduction in the decay matrix element at higher photon energies.[13,39]

The decay matrix elements for peaks A (LUMO) and D (LUMO+1), which are governed by the Coulomb operator $-e^2/r$, are given by the following expressions, in which the states that participate in the decay are indicated by their occupation number relative to the ground state occupation (k indicates the wave vector of the emitted electron):

$$\begin{aligned}\left\langle (\mathrm{HOMO})^{-1} k \left| \frac{1}{r} \right| 1s^{-1} (\mathrm{LUMO})^{1} \right\rangle &\propto \frac{I_{\mathrm{RPES}}^{\mathrm{multi}}}{I_{\mathrm{XAS}}^{\mathrm{multi}}} (\mathrm{LUMO}) \\ &\equiv \sigma_{\mathrm{LUMO}}, \\ \left\langle (\mathrm{HOMO})^{-1} k \left| \frac{1}{r} \right| 1s^{-1} (\mathrm{LUMO}+1)^{1} \right\rangle &\propto \frac{I_{\mathrm{RPES}}^{\mathrm{multi}}}{I_{\mathrm{XAS}}^{\mathrm{multi}}} (\mathrm{LUMO}+1) \\ &\equiv \sigma_{\mathrm{LUMO}+1}.\end{aligned} \tag{1}$$

We thus define σ_{LUMO} and $\sigma_{\mathrm{LUMO}+1}$ as the intensity ratios between the RPES and the XAS lines of the indicated resonances. By virtue of the normalization to the lowest resonance as outlined earlier, σ_{LUMO} is one for both molecules. This is justified since we are interested only in the variation as a function of resonance being excited for a given molecule, and not in absolute intensities. Then $\sigma_{\mathrm{LUMO}+1} = 0.33\,(0.30)$ for isonicotinic acid (bi-isonicotinic acid). The change in size of the matrix elements is then easily motivated by an increase in spatial extent of the participating orbitals at higher energies, and from the equations it is seen that the Coulomb operator-modified overlap of highest occupied molecular orbital (HOMO) and LUMO and HOMO and LUMO+1, respectively, is responsible for the decrease. Note that symmetry effects must be considered as well, and that the present arguments are meant as a first-order description of likely behavior. A similar argument applies to the hydrogen-bonded LUMO (peak HB-A) relative to the LUMO. If intermolecular hopping were important for the multilayer resonances D (for resonance A it is certain that the excited electron is localized on the molecule as outlined earlier), then the factors 0.33 (isonicotinic acid) and 0.30 (bi-isonicotinic acid) used in the following would increase proportionally. The rates derived in the following for the excited state charge transfer in the monolayers must therefore be considered as upper limits.

B. Monolayer resonant photoemission

A similar comparison is presented in Fig. 6 for the monolayer data. Here, the integration boundaries were set to 7 and 11 eV binding energy, which means that states are monitored which correspond to the multilayer measurement. Concerning the shapes of the x-ray absorption spectra, the case of isonicotinic acid differs from that of bi-isonicotinic acid mainly in the character of the second resonance (C vs B). While B of bi-isonicotinic acid is of π-character[9,40] and obtains the observed energetic position by the interaction of the molecule with the substrate,[40] resonance C of isonicotinic acid is attributed to an intermolecular interaction arising from the constraints of the molecular adsorption geometry.[18] Resonance D (the LUMO+2) of the monolayer corresponds to the LUMO+1 of the multilayer,[40] also labeled D.

The qualitative estimation for Fig. 4(d), that no RPES intensity is observed for the higher resonances, applies also

quantitatively down to the present level of noise. Assuming that the maximum RPES signal for peak D is given by the noise N, this signal amounts to less than 15% (10%) of the corresponding XAS signal S for isonicotinic acid (bi-isonicotinic acid), i.e., $I_{\mathrm{RPES}}^{\mathrm{mono}}/I_{\mathrm{XAS}}^{\mathrm{mono}}<0.15$ for isonicotinic acid (0.10 for bi-isonicotinic acid). Knowledge of the relative decrease in Coulombic matrix element when passing from the LUMO (resonance A) to the (multilayer) LUMO+1 (resonance D), which as shown above is given by $\sigma_{\mathrm{LUMO+1}}$, enables one then to estimate the excited electron transfer time τ_{CT} for excitation to resonance D from the core-hole lifetime τ_C by rearranging equations given in Ref. 13 (observe that the LUMO+2 of the monolayer corresponds to the LUMO+1 of the multilayer, both labeled D, which necessitates the use of $\sigma_{\mathrm{LUMO+1}}$),

$$\tau_{\mathrm{CT}}=\tau_C\frac{\dfrac{I_{\mathrm{RPES}}^{\mathrm{mono}}}{I_{\mathrm{XAS}}^{\mathrm{mono}}}}{\sigma_{\mathrm{LUMO+1}}-\dfrac{I_{\mathrm{RPES}}^{\mathrm{mono}}}{I_{\mathrm{XAS}}^{\mathrm{mono}}}}. \tag{2}$$

Replacing the intensity ratios by the above-specified values and in Sec. IV A and setting $\tau_C=6$ fs (Ref. 41), the upper limits are

$\tau_{\mathrm{CT}}<5$ fs, isonicotinic acid,

$\tau_{\mathrm{CT}}<3$ fs, bi-isonicotinic acid.

On the basis of its substrate bond character,[40] we estimate for resonance B of bi-isonicotinic acid that $\tau_C<3$ fs, as well, assuming that the matrix element is similar to that of resonance D.

We would like to emphasize that the present method allows one to determine not only upper limits to the charge transfer times, but, within proper error margins, defined ranges for these times, whose accuracy is limited only by the uncertainty in the core hole lifetime.[13] Here, a lower limit is not available, since the present level of noise does not allow us to specify the RPES signal intensities for the resonances D. This shortcoming could in principal be overcome by longer measuring times, which, however, in the present case turned out to be prohibitively long.

C. Monolayer resonant Auger

Above it has been touched upon that the most reliable method of measuring charge transfer times with the help of resonant core spectroscopies is to identify the resonant (RAES+RPES) and nonresonant (normal Auger) parts of the decay spectra and to calculate the charge transfer time from the branching ratio of the resonant channel.[13] This method has been successfully applied to small molecules (CO, N_2, and noble gases) adsorbed on various metallic and semimetallic surfaces and to multilayers of the noble gases.[12,21,35,42,43]

Most of the resonant intensity is contained in the resonant Auger features, while the resonant photoemission contribution often can be neglected relative to the former. Thus, to first order, the branching ratio can be accurately estimated using the ratio of the resonant Auger and normal Auger parts of the spectrum only. The resonant and nonresonant parts of the spectrum can then be distinguished from each other by the spectator shift mentioned in Sec. IV, or in favorable cases by using the Auger resonant Raman condition. In less complex molecular systems the shift is either large enough [e.g., larger than 10 eV for the lowest excitations in N_2 and N_2O (Refs. 44 and 21)] or the valence electronic structure is sufficiently simple (that is the case in, e.g., Ar, where the spectator shift amounts to only a few electron volts[35]) to allow an unambiguous identification of the intensities of the different channels. In organic molecules, and in particular aromatic compounds, the screening efficiency of the π-system[45] leads to relatively small spectator shifts, for example, 3–4 eV in benzene,[46] 2.5 eV (C K-edge) and 4.0 eV (N K-edge) in pyrrole,[47] and 4 eV in pyridine, pyrazine, and s-triazine.[48] Due to a complicated valence electronic structure, the nonresonant and resonant Auger features then overlap, rendering a positive identification very difficult.

Such an identification can nevertheless be accomplished using the off-resonantly measured normal Auger spectrum, the shape of which is a good approximation to that of the resonant Auger spectrum. In the present case the interest lies in obtaining a N KVV Auger spectrum which can be compared to the N 1s resonant spectra. The measurement is hampered by the presence of the substrate Ti atoms, since the Ti LVV Auger excited above approximately 455 eV photon energy appears at the same kinetic energies as those of the N KVV spectrum, and has a similar shape. Thus, the measurement has to be conducted at photon energies well above the N absorption edge at around 400 eV and below the Ti 2p absorption edge at around 455 eV. At these energies, the Ti 3p and Ti 3s direct valence photoemission features with rich shake-up structures as well the O 1s direct photoemission peak excited with second-order light disturb the acquisition. This is illustrated by the top curve in Fig. 7. Since the involved substrate line shapes changed an undetermined amount upon adsorption of the bi-isonicotinic acid, a reliable Auger curve was not obtainable by subtracting a clean crystal spectrum from that of the monolayer. Instead, another approach was chosen that is also illustrated in Fig. 7. The Ti 3s direct photoemission peak, which is given for a photon energy of 438 eV in the inset of Fig. 7, was measured repeatedly at a large number of photon energies between 423 and 455 eV. The manifold of these spectra is given in the middle of Fig. 7. The envelope of these curves, given in the lower part of the figure, then gives a relatively good approximation to the true Auger line shape (cf. the topmost and the lowermost curves in Fig. 7).

The resonant spectra for a monolayer of bi-isonicotinic acid adsorbed on rutile $TiO_2(110)$ measured at the maxima of the x-ray absorption spectrum (Fig. 6) are given in Fig. 8. The Auger curve of Fig. 7 has been added to these graphs. In order to explain the resonant intensity for excitation to the LUMO [resonance A, panel (a)], the Auger curve has to be shifted to higher kinetic energies, corresponding to an estimated spectator shift of approximately 3 eV. The remaining intensity can then be explained by direct photoemission and resonant photoemission features. This finding corresponds well to the excited electron localization observed from the

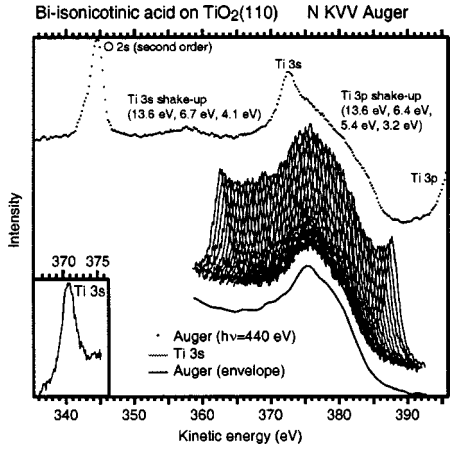

FIG. 7. Normal Auger measurement for bi-isonicotinic acid on rutile $TiO_2(110)$. The upper curve shows a typical Auger measurement at 440 eV photon energy which is overlaid by the indicated direct photoemission features. Since the photon energy has to be kept between approximately 420 and 455 eV (see the text), these peaks are always present in the measurement. In order to obtain a reasonably reliable Auger measurement, the Ti 3*s* core level was measured at a large number of photon energies between 430 and 455 eV photon energy. These spectra are presented in the middle of the figure, while the inset shows one of these curves separately (photon energy 438 eV). The envelope of this set of spectra (lower spectrum) represents the Auger curve, slightly modified by the slowly changing cross sections of the substrate background, Ti 3*s*, and adsorbate N 1*s* levels, the latter of which gives rise to the Auger signal.

electronic structure determination in Sec. III and the resonant photoemission data. It should be noted that the shifted Auger curve representing the resonant Auger seems to overestimate the resonant intensity at kinetic energies around 390 eV. Due to the gap between HOMO and LUMO no Auger intensity should be observed this close to the HOMO.

It is more difficult to evaluate the situation for excitation to the LUMO+1 and the LUMO+2 [resonances B and D, panels (b) and (c) of Fig. 8], and thus these figures can serve as an illustration of the problems in distinguishing between resonant and nonresonant Auger mentioned earlier. The main part of the intensity seems to be well explained by the nonshifted Auger curve, and thus the resonant photoemission results are confirmed, that the excited electron delocalizes rapidly into the substrate. From the data, however, it is impossible to fully exclude a shifted resonant component. The use of the resonant photoemission features only as shown in Sec. IV B thus gives a much more reliable account of the extent of localization or delocalization of the excited electron.

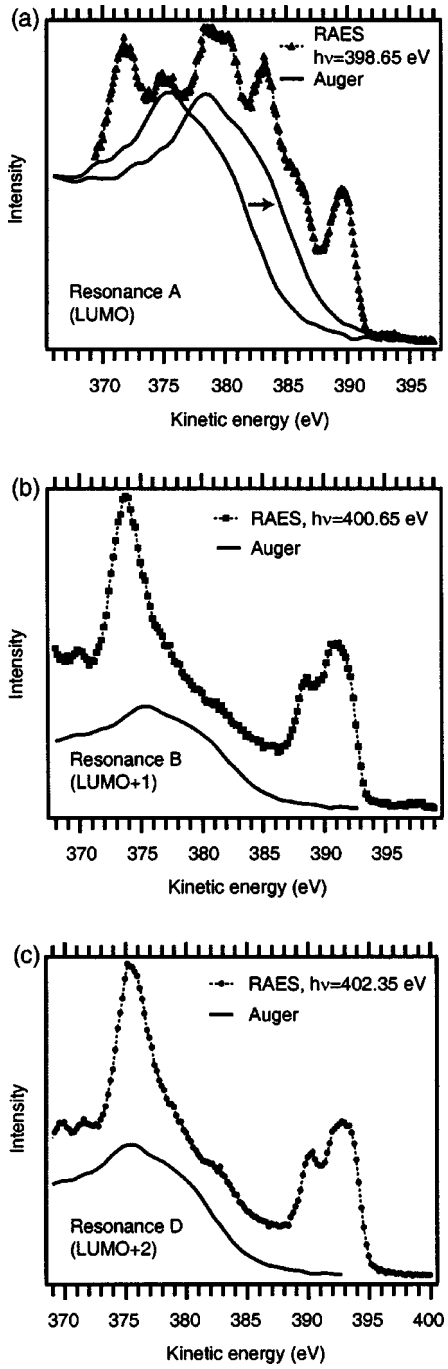

FIG. 8. Resonant Auger spectra for a monolayer of bi-isonicotinic acid on $TiO_2(110)$ excited at resonances A, B, and D. The solid line represents the N *KVV*-Auger. In (a) an estimate of the spectator shift has been indicated by shifting the Auger curve to higher kinetic energies by 3 eV, so that good agreement is achieved for the spectral shapes. The samples of panels (b) and (c) were slightly Ta-contaminated which can be seen from the double-peak Ta 4*f* structure at around 370 eV kinetic energy. From the intensities and the ionization cross sections of the Ta 4*f* and O 2*s* structures it is estimated that the Ta coverage lay below one Ta atom per hundred surface unit cells.

V. DISCUSSION

The results show that the binding of the isonicotinic acid and bi-isonicotinic acid adsorbates to the TiO_2 substrate via the carboxylic group allow for a very rapid delocalization of the excited electron into the substrate if the requirement of an energetic level matching of the adsorbate and substrate states is fulfilled. The finding of low-fs upper limits for the charge transfer times across the interface helps to rationalize the ultrafast electron transfer for the N3 dye itself.[3–8]

There exist a number of differences between the experiments on the $N3/TiO_2$ system and the present one. Systeminherent are the different sizes of the N3 molecule and the bi-isonicotinic acid ligand and the isonicotinic acid molecule studied here. Recent results achieved with resonant core techniques[49] indicate that intramolecular delocalization within the N3 metallo-organic complex limits the resolution of the technique, leaving open the question of the charge

transfer time as measured by the present technique for N3. However, it is important also to note that the results of Ref. 49 are consistent with the present results within the uncertainties.

Another important difference concerns the type of excitation employed. As is apparent in a time-dependent picture of the resonant excitation process, the photon field can be considered to pump the system at the given photon frequency.[50,51] The so-prepared excited state follows a coherent time development which for the isolated molecule includes the evolution of the excited state along the appropriate potential energy surface, a decay term to the final state, and (for narrow-band excitation only) the ongoing pumping induced by the photon field.[50,51] In addition, in the coupled adsorbate/substrate system the charge transfer has to be taken into account, which quenches the coherence[13,52] at a frequency corresponding approximately to the inverse charge transfer bandwidth (see, e.g., Ref. 53). Important in this picture is that the charge transfer cannot be resolved if it proceeds on a shorter or comparable time scale than defined by the excitation frequency. For soft x-ray frequencies this introduces no complication since the excitation frequency is much higher than the upper limits for the charge transfer frequencies derived above (for $h\nu = 400\,\mathrm{eV}$ typical for our experiments the light frequency is $9.7\times10^{16}\,\mathrm{Hz}$, which corresponds to approximately 10 as; the upper limits for the charge transfer correspond to $2.0\times10^{14}\,\mathrm{Hz}$ [(isonicotinic acid) and $3.3\times10^{14}\,\mathrm{Hz}$ (bi-isonicotinic acid)]. For optical frequencies (i.e., frequencies in the visible or near-visible range), by contrast, the excitation frequency is comparable to the frequencies which correspond to the given upper limits (for $\lambda = 700$ nm the optical frequency is $4.3\times10^{14}\,\mathrm{Hz}$ comparable to the charge transfer frequencies above).

It is thus more general to discuss the adsorbate-substrate interaction in terms of coupling strength or an electron transfer bandwidth.[10] From the low-fs charge transfer time scale found here, we can conclude that the interface is characterized by a strong interfacial electronic coupling and the transfer proceeds in the electronic limit.[54] This coupling allows for excited transfer processes that suppress the competing processes of intramolecular charge redistribution[55,56] (in the N3 complex) and intramolecular thermalization.[57–59] The virtual equivalency of the results for isonicotinic acid and bi-isonicotinic acid also suggests that the details of how N3 bonds to the substrate (i.e., via one[60,61] or two[62,63] dcb ligands) is not likely to be crucial for the gross electron transfer properties from the point of view of the ligand coupling strength.

Interestingly, the structure of the (crystalline) substrate has been found to have little influence on the charge transfer rate from bi-isonicotinic acid to TiO_2-adsorption on nanostructured anatase leads to a rate in the same range as that found here.[64] This can partly be understood from the similar bonding geometries[9,61,64] for bi-isonicotinic acid on the relevant rutile and anatase surfaces, which also leads to similar electronic structure.[64] Given the large number of substrates of interest for electrochemical and photochemical applications, there are many systems which could be explored using the present method, with a number of pump–probe studies with which to compare.[3,6,65–67]

Of principal impact on the results is the existence of a core hole on the adsorbate. This can be read from the placement of the lowest resonance within the substrate band gap, whereas the LUMO (which is the orbital that corresponds to the lowest resonance) in its ground state would overlap the conduction band.[40,68] Since optical excitations result in very similar excitonic effects this effect is not a fundamental drawback of the core techniques employed here. In particular, available data for aromatic π systems indicate that the excitonic binding energies are actually very similar for core and valence holes.[45] The initial excitation in the N3 complex is, however, a metal-to-ligand charge transfer excitation, the effect of which on the ligand states will need to be explored, but which is expected to be reduced by screening from the other ligands. An excitonic effect could be expected to be more important in other, smaller sensitizers. Indeed, this issue would appear to be central in the comparison of our results [especially Fig. 2(b)] with the calculations of Ref. 69. There the HOMO–LUMO excitation is calculated to lie in the conduction band, as opposed to being in the band gap. We can only speculate that this is due to the neglect of well-known self-energy effects in the time-dependent local density approximation used there. The further conflict in the charge transfer times found is not possible for us to understand at this time, but it would be interesting to see the results of the same formalism applied to the CO/Ru(0001) system which has a similar short charge transfer time.[12]

Since a very low charge transfer time constant (6 fs) has been found for alizarin on TiO_2 nanoparticles[67] and recent calculations predict similarly short time scales for electron injection from catechol into TiO_2 (Ref. 70), two molecules comparable in size to the present acids, it seems that the hole–electron interaction does not influence the transfer appreciably as long as the electronic matching is good. In the light of these arguments, the present results should also give a good account of the coupling strength of the N3 complex to the TiO_2 substrate.

VI. CONCLUSIONS

Resonant core spectroscopies have been used to study the excited-state charge transfer dynamics in systems of aromatic molecules on a low-femtosecond time scale. The systems studied comprise multilayers of isonicotinic acid and bi-isonicotinic acid as well as monolayers of these molecules adsorbed on rutile $TiO_2(110)$. Since the multilayers condense as van der Waals-bound molecular crystals, the data obtained on these films correspond to those of the isolated molecule. Thus, the multilayers can be used to obtain information on the size of the excited state-dependent decay matrix elements. In the monolayers, the excited electron is localized on the adsorbate by an excitonic effect for excitation to the lowest resonance. The next two higher resonances overlap the substrate conduction band, and upper limits for the observed electron transfer are specified to 5 fs (isonicotinic acid) and 3 fs (bi-isonicotinic acid). This shows that a single pyridine carboxylic acid group is sufficient to provide a highly efficient electron conduit into the (110) rutile[10] and

likely also anatase nanoparticle[64] surfaces, consistent with direct electronic coupling of the unoccupied levels to the substrate conduction band.[54]

The results have been obtained by the application of a novel method of resonant photoemission, previously applied at a few selected energies, but here over a grid of energies in the XAS edge region. This allows one to isolate the resonant signal, which corresponds to a localization of the excited electron, from an interfering substrate background and the nonresonant parts of the spectrum. The method allows one to obtain significant information on the charge transfer dynamics even in cases in which the complicated structure of the decay spectra does not allow a straightforward separation of the resonant and nonresonant spectral features. For larger systems, the weaker resonant signal will place higher demands on the statistics of the spectra, but the access to very short times and the chemical specificity of the technique offer significant rewards when the method can be applied.

ACKNOWLEDGMENTS

We would like to acknowledge J.-O. Forsell, L. Bolkegård, and L. Ekberg for technical support, S. Södergren, M. Bässler, and H. Hillesheimer for help during some of the experiments, the staff at MAX-Lab, in particular K. Hansen, S. Wiklund, R. Nyholm, and M. Leandersson, for assistance in the experimental work, and our funding sources Vetenskapsrådet, Göran Gustafssons stiftelse, and the CARAMEL Consortium, which is funded by Stiftelsen för Strategisk Forskning.

[1] A. Hagfeldt and M. Grätzel, Acc. Chem. Res. **33**, 269 (2000).
[2] M. K. Nazeeruddin, A. Kay, I. Rodicio, R. Humphry-Baker, E. Müller, P. Liska, N. Vlachopoulos, and M. Grätzel, J. Am. Chem. Soc. **115**, 6382 (1993).
[3] Y. Tachibana, J. E. Moser, M. Grätzel, D. R. Klug, and J. R. Durrant, J. Phys. Chem. **100**, 20056 (1996).
[4] T. Hannappel, B. Burfeindt, W. Storck, and F. Willig, J. Phys. Chem. B **101**, 6799 (1997).
[5] J. B. Asbury, E. Hao, Y. Wang, H. N. Ghosh, and T. Lian, J. Phys. Chem. B **105**, 4545 (2001).
[6] T. A. Heimer, E. J. Heilweil, C. A. Bignozzi, and G. J. Meyer, J. Phys. Chem. A **104**, 4256 (2000).
[7] G. Benkö, J. Kallioinen, J. E. I. Korppi-Tommola, A. P. Yartsev, and V. Sundström, J. Am. Chem. Soc. **124**, 489 (2002).
[8] J. Kallioinen, G. Benkö, V. Sundström, J. E. I. Korppi-Tommola, and A. P. Yartsev, J. Phys. Chem. B **106**, 4396 (2002).
[9] L. Patthey, H. Rensmo, P. Persson *et al.*, J. Chem. Phys. **110**, 5913 (1999).
[10] J. Schnadt, P. A. Brühwiler, L. Patthey *et al.*, Nature (London) **418**, 620 (2002).
[11] For reasons of continuity with our previous publication (Ref. 10) we adopt a terminology in which the term ''resonant photoemission'' is used for describing a process (the participant decay) for which the final state is the same as that of a direct valence photoemission event. We reserve the term ''resonant Auger'' for describing the so-called spectator decay, in which the excited electron does not take part in the deexcitation. In the literature these two terms are normally not defined in this strict manner.
[12] C. Keller, M. Stichler, G. Comelli, F. Esch, S. Lizzit, W. Wurth, and D. Menzel, Phys. Rev. Lett. **80**, 1774 (1998).
[13] P. A. Brühwiler, O. Karis, and N. Mårtensson, Rev. Mod. Phys. **74**, 703 (2002).
[14] O. Karis, A. Nilsson, M. Weinelt, T. Wiell, C. Puglia, N. Wassdahl, N. Mårtensson, J. Stöhr, and M. Samant, Phys. Rev. Lett. **76**, 1380 (1996).
[15] M. Weinelt, A. Nilsson, M. Magnuson, T. Wiell, N. Wassdahl, O. Karis, A. Föhlisch, N. Mårtensson, J. Stohr, and M. Samant, Phys. Rev. Lett. **78**, 967 (1997).
[16] P. A. Brühwiler, A. J. Maxwell, P. Rudolf, C. D. Gutleben, B. Wästberg, and N. Mårtensson, Phys. Rev. Lett. **71**, 3721 (1993).
[17] A. J. Maxwell, P. A. Brühwiler, D. Arvanitis, J. Hasselström, and N. Mårtensson, Phys. Rev. Lett. **79**, 1567 (1997).
[18] J. Schnadt, J. Schiessling, J. N. O'Shea *et al.*, Surf. Sci. **540**, 39 (2003).
[19] J. Schnadt, J. N. O'Shea, L. Patthey, J. Schiessling, J. Krempaský, M. Shi, N. Mårtensson, and P. A. Brühwiler, Surf. Sci. **544**, 74 (2003).
[20] W. Wurth, C. Schneider, R. Treichler, E. Umbach, and D. Menzel, Phys. Rev. B **35**, 7741 (1987).
[21] O. Björneholm, A. Nilsson, A. Sandell, B. Herrnäs, and N. Mårtensson, Phys. Rev. Lett. **68**, 1892 (1992).
[22] R. Denecke, P. Väterlein, M. Bässler, N. Wassdahl, S. Butorin, A. Nilsson, J.-E. Rubensson, J. Nordgren, N. Mårtensson, and R. Nyholm, J. Electron Spectrosc. Relat. Phenom. **101–103**, 971 (1999).
[23] J. N. Andersen, O. Björneholm, A. Sandell, R. Nyholm, J. Forsell, L. Thånell, A. Nilsson, and N. Mårtensson, Synchrotron Radiat. News **4**(4), 15 (1991).
[24] J. Schnadt, J. N. O'Shea, L. Patthey, J. Krempaský, N. Mårtensson, and P. A. Brühwiler, Phys. Rev. B **67**, 235420 (2003).
[25] See, e.g., the discussion in Sec. IV of R. Ahuja, P. A. Brühwiler, J. M. Willis, B. Johansson, N. Mårtensson, and O. Eriksson, Phys. Rev. B **54**, 14396 (1994).
[26] D. C. Cronemeyer, Phys. Rev. **87**, 876 (1952).
[27] J. Purton, D. W. Bullett, P. M. Oliver, and S. C. Parker, Surf. Sci. **336**, 166 (1995).
[28] K. M. Glassford and J. R. Chelikowsky, Phys. Rev. B **46**, 1284 (1992).
[29] P. K. Schelling, N. Yu, and J. W. Halley, Phys. Rev. B **58**, 1279 (1998).
[30] F. M. F. de Groot, J. Faber, J. J. M. Michiels, M. T. Czyźyk, M. Abbate, and J. C. Fuggle, Phys. Rev. B **48**, 2074 (1993).
[31] G. van der Laan, Phys. Rev. B **41**, 12366 (1990).
[32] A. K. See and R. A. Bartynski, J. Vac. Sci. Technol. A **10**, 2591 (1992).
[33] F. Gel'mukhanov and H. Ågren, Phys. Rep. **312**, 87 (1999).
[34] G. S. Brown, M. H. Chen, B. Crasemann, and G. E. Ice, Phys. Rev. Lett. **45**, 1937 (1980).
[35] W. Wurth and D. Menzel, Chem. Phys. **251**, 141 (2000).
[36] Choosing to integrate over the same states as in the monolayer, which would correspond to setting the integration boundaries to 7.3 and 11.3 eV, results in virtually the same curve as given here.
[37] J. N. O'Shea, J. Schnadt, P. A. Brühwiler, H. Hillesheimer, N. Mårtensson, L. Patthey, J. Krempaský, C. K. Wang, Y. Luo, and H. Ågren, J. Phys. Chem. B **105**, 1917 (2001).
[38] J. N. O'Shea, Y. Luo, J. Schnadt, L. Patthey, H. Hillesheimer, J. Krempaský, D. Nordlund, M. Nagasano, P. A. Brühwiler, and N. Mårtensson, Surf. Sci. **486**, 157 (2001).
[39] P. A. Brühwiler, A. J. Maxwell, A. Nilsson, R. L. Whetten, and N. Mårtensson, Chem. Phys. Lett. **193**, 311 (1992).
[40] P. Persson, S. Lunell, P. A. Brühwiler *et al.*, J. Chem. Phys. **112**, 3945 (2000).
[41] B. Kempgens, A. Kivimäki, M. Neeb, H. M. Köppe, A. M. Bradshaw, and J. Feldhaus, J. Phys. B **29**, 5389 (1996).
[42] A. Sandell, O. Hjortstam, A. Nilsson, P. A. Brühwiler, O. Eriksson, P. Bennich, P. Rudolf, J. M. Wills, B. Johansson, and N. Mårtensson, Phys. Rev. Lett. **78**, 4994 (1997).
[43] C. Keller, M. Stichler, G. Comelli, F. Esch, S. Lizzit, D. Menzel, and W. Wurth, Phys. Rev. B **57**, 11951 (1998).
[44] F. P. Larkins, W. Eberhardt, I.-W. Lyo, R. Murphy, and E. W. Plummer, J. Chem. Phys. **88**, 2948 (1988).
[45] J. Schnadt, J. Schiessling, and P. A. Brühwiler (unpublished).
[46] D. Menzel, G. Rocker, H.-P. Steinrück, D. Coulman, P. A. Heimann, W. Huber, P. Zebisch, and D. R. Lloyd, J. Chem. Phys. **96**, 1724 (1992).
[47] M. Mauerer, P. Zebisch, M. Weinelt, and H.-P. Steinrück, J. Chem. Phys. **99**, 3343 (1993).
[48] R. Dudde, M. L. M. Rocco, E. E. Koch, S. Bernstorff, and W. Eberhardt, J. Chem. Phys. **91**, 20 (1989).
[49] K. Westermark, H. Rensmo, J. Schnadt, P. Persson, S. Södergren, P. A. Brühwiler, S. Lunell, and H. Siegbahn, Chem. Phys. **285**, 167 (2002).
[50] E. Pahl, H.-D. Meyer, and L. S. Cederbaum, Z. Phys. D: At., Mol. Clusters **38**, 215 (1996).
[51] Z. W. Gortel, R. Teshima, and D. Menzel, Phys. Rev. A **58**, 1225 (1998).
[52] Z. W. Gortel and D. Menzel, Phys. Rev. B **64**, 115416 (2001).
[53] M. Ohno, Phys. Rev. B **50**, 2566 (1994).
[54] J. M. Lanzafame, S. Palese, D. Wang, R. J. D. Miller, and A. A. Muenter, J. Phys. Chem. **98**, 11020 (1994).
[55] A. T. Yeh, C. V. Shank, and J. K. McCusker, Science **289**, 935 (2000).

[56] Y. Tachibana, S. A. Haque, I. P. Mercer, J. R. Durrant, and D. R. Klug, J. Phys. Chem. B **104**, 1198 (2000).
[57] N. H. Damrauer, G. Cerullo, A. Yeh, T. R. Boussie, C. V. Shank, and J. K. McCusker, Science **275**, 54 (1997).
[58] V. Blanchet, M. Z. Zgierski, T. Seideman, and A. Stolow, Nature (London) **401**, 52 (1999).
[59] F. Willig, C. Zimmermann, S. Ramakrishna, and W. Storck, Electrochim. Acta **45**, 4565 (2000).
[60] H. Rensmo, K. Westermark, S. Södergren, O. Kohle, P. Persson, S. Lunell, and H. Siegbahn, J. Chem. Phys. **111**, 2744 (1999).
[61] P. Persson and S. Lunell, Sol. Energy Mater. Sol. Cells **63**, 139 (2000).
[62] V. Shklover, Y. E. Ovchinnikov, L. S. Braginsky, S. M. Zakeeruddin, and M. Grätzel, Chem. Mater. **10**, 2533 (1998).
[63] A. Fillinger and B. A. Parkinson, J. Electrochem. Soc. **146**, 4559 (1999).
[64] J. Schnadt, A. Henningsson, M. P. Andersson, P. G. Karlsson, P. Uvdal, H. Siegbahn, P. A. Brühwiler, and A. Sandell, J. Phys. Chem. B. (to be published).
[65] R. J. Ellingson, J. B. Asbury, S. Ferrere, H. N. Gosh, J. R. Sprague, T. Lian, and A. J. Nozik, J. Phys. Chem. B **102**, 6455 (1998).
[66] J. B. Asbury, R. J. Ellingson, H. N. Gosh, S. Ferrere, A. J. Nozik, and T. Lian, J. Phys. Chem. B **103**, 3110 (1999).
[67] R. Huber, J.-E. Moser, M. Grätzel, and J. Wachtveitl, J. Phys. Chem. B **106**, 6494 (2002).
[68] M. Odelius (private communication).
[69] W. Stier and O. V. Prezhdo, J. Phys. Chem. B **106**, 8047 (2002).
[70] L. G. C. Rego and V. S. Batista, J. Am. Chem. Soc. **125**, 7989 (2003).